
**ELECTRODYNAMICS
AND WAVE PROPAGATION**

Diffraction of a Cylindrical Wave by a Perfectly Conducting Cylinder Enclosed in a Metamaterial Shell with a Negative Refractive Index

A. P. Anyutin

Russian New University, ul. Radio 22, Moscow, 105005 Russia

e-mail: anioutine@mail.ru

Received June 1, 2013

Abstract—The problem of diffraction of a plane (cylindrical) wave by a perfectly conducting cylinder enclosed in a metamaterial shell is rigorously solved. The influence of the geometric dimensions of the shell, the value of the negative refractive index of the metamaterial medium, and the position of a cylindrical wave source on the field structure in the near zone of the scatterer is investigated. It is found that, in the quasi-optical range of the problem parameters, this structure does not exhibit ideal focusing. It is shown that, there are two types of caustics inside the shell. The first type is related with rays reflected by the surface of the interior cylinder and has one cusp point, and the second type is formed by the geometric-optics rays that are refracted by the outer boundary of the shell and do not fall on the surface of the interior perfectly conducting cylinder. The spatial distribution of the total field amplitude and of the equal-amplitude lines in the near zone of the scatterer is reported. The obtained numerical results are correctly interpreted from the physical viewpoint.

DOI: 10.1134/S106422691401001X

INTRODUCTION

In the recent decade, the interest in problems of wave diffraction by compact metamaterial bodies characterized by negative relative permittivity $\epsilon_r < 0$ and negative relative permeability $\mu_r < 0$ (a negative refractive index) has increased. Note that the pioneer study where extraordinary (from the viewpoint of ordinary media) effects of interaction of plane and cylindrical waves with a homogeneous medium layer with a negative refractive index were predicted was published in 1967 [1], and an experimental observation of these effects was first reported in 2000 [2]. The number of studies considering various aspects of interaction of waves with such a medium permanently has been growing every year starting from 2000.

The methods used for solving the corresponding problems of diffraction of electromagnetic waves by compact metamaterial bodies include the geometric optics (GO) method, the Kirchhoff approximation, the Fourier method, the finite element method, and the modified method of discrete sources (MMDS) [3–13, 18]. However, we should note that many publications exhibit features of advertising materials and contain a number of unjustified statements. For example, certain studies state that a 2D structure consisting of a perfectly conducting cylinder covered by a finite layer of a homogeneous metamaterial with the relative permittivity $\epsilon_r = -1$ and the relative permeability $\mu_r = -1$ ideally focuses an incident plane wave in the interior and exterior of the metamaterial. From the

GO viewpoint, this means that the GO rays refracted and reflected by the structure form an ideal focus in the both interior and exterior of the shell by analogy with a plane Veselago lens (see [4, 5] and the references cited therein).

In this study, it is shown that, when a plane wave is diffracted by such a structure, an ideal GO focus is not formed but there are caustics of rays refracted and reflected by the perfectly conducting cylinder and that these caustics can have a cusp point. The amplitudes of the refracted and scattered fields increase near such caustics. In addition, we present and discuss examples of the solution of the problem of diffraction of a cylindrical wave by this structure for various positions of the cylindrical wave source.

1. FORMULATION OF THE PROBLEM AND DISCUSSION OF RESULTS

Consider the 2D problem of scattering of cylindrical wave $U_0(r, \varphi)$:

$$U_0(r, \varphi) = H_0^{(2)}(k\sqrt{r^2 + R_0^2 - 2rR_0 \cos(\varphi - \varphi_0)}) \quad (1)$$

by a perfectly conducting cylinder of radius a_0 enclosed in a metamaterial shell of thickness d . The outer radius of the shell is $a_1 = a_0 + d$. The axis of the metal cylinder coincides with the axis of the cylindrical shell (Fig. 1). In addition, it is assumed that the shell's medium has relative permittivity $\epsilon_r < 0$ and relative permeability $\mu_r < 0$, i.e., is a metamaterial with

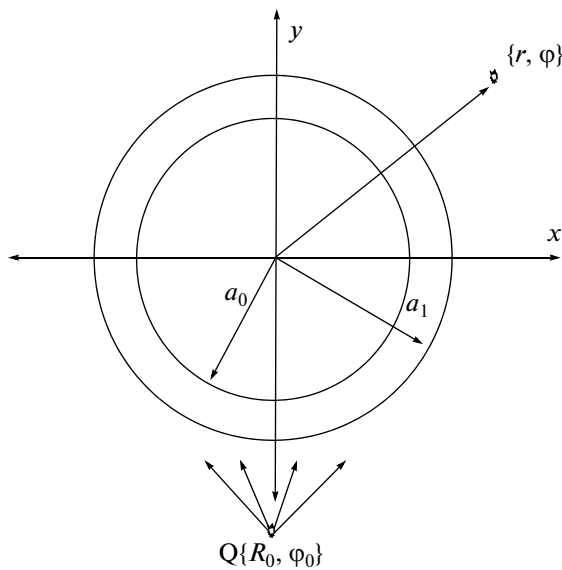


Fig. 1. Geometry of the problem.

the negative refractive index $n_r = -\sqrt{\epsilon_r |\mu_r|} - i\nu$, where quantity ν characterizes the medium loss.

Expression (1) contains the following quantities: cylindrical spatial coordinates $\{r, \varphi\}$ of the observation point, cylindrical spatial coordinates $\{R_0, \varphi_0\}$ of the point of wave source Q , wave number of free space k , zero-order Hankel function of the second kind $H_0^{(2)}(\cdot)$, and parameters a and d characterizing the geometry of the scattering structure.

Total field $U(r, \varphi)$ beyond the shell can be represented as the superposition of incident wave field (1) and scattered field $U_1(r, \varphi)$ in the form

$$U(r, \varphi) = H_0^{(2)} \left(k\sqrt{r^2 + R_0^2 - 2rR_0 \cos(\varphi - \varphi_0)} \right) + U_1(r, \varphi). \quad (2)$$

We denote the field in the metamaterial $U_2(r, \varphi)$.

As is known, fields $U(r, \varphi)$ and $U_2(r, \varphi)$ satisfy the corresponding Helmholtz equations in the exterior and interior of the shell and the corresponding boundary conditions on contours $\rho_0(\varphi) = a_0$ and $\rho_1(\varphi) = a_1$ of the shell (see Fig. 1). To solve numerically this boundary value problem, we apply the MMDS [16, 17], which enables us to obtain a solution with a controlled accuracy. In this method, fields $U_1(r, \varphi)$ and $U_2(r, \varphi)$ are represented as a superposition of the fields produced by auxiliary cylindrical wave sources located on auxiliary contours $\rho_{\Sigma 11}(\varphi)$, $\rho_{\Sigma 21}(\varphi)$, and $\rho_{\Sigma 22}(\varphi)$ inside and beyond contours $\rho_0(\varphi)$ and $\rho_1(\varphi)$. This representation automatically satisfies the Helmholtz equations and the Sommerfeld condition.

In the MMDS, the amplitude coefficients for the fields of auxiliary cylindrical wave sources are found

from the boundary conditions fulfilled at N points of each of contours $\rho_1(\varphi)$ and $\rho_0(\varphi)$.

The accuracy of the solution to the problem is controlled through calculating the discrepancy of the boundary conditions at the centers of the intervals between the points where the boundary conditions are fulfilled exactly. At the aforementioned centers of intervals, the boundary conditions are satisfied with the worst accuracy [17].

The MMDS and the technique of its application to a number of problems with a similar configuration of a scatterer's contour are described in detail in [16, 17]. Therefore, we will not discuss the peculiarities of the MMDS application in the case under consideration and only note that the scattering patterns presented below are calculated with the maximum discrepancy of the boundary conditions that does not exceed the quantity $\Delta < 10^{-3}$ for any point of the corresponding contours.

First, let us consider the problem of diffraction of cylindrical wave (1) by a perfectly conducting cylinder that has the electric radius $ka_0 = 6$ and is enclosed in a metamaterial shell. The outer electric radius of the shell is $ka = 10$. Thus, the electric thickness $kd = ka - ka_0$ of the shell is assumed to be $kd = 4$, i.e., we deal to with the case of a relatively thin shell. The cylindrical wave source has the coordinates $kR_0 = 700$ and $\varphi_0 = \pi$. Physically, this means that the cylindrical wave source is located in the far zone of the scatterer and the incident wave has a plane front. Note that overall dimension kD of the shell satisfies the condition $kD = 2ka = 20 \gg 1$, though the shell's thickness is smaller than the wavelength. Assume that the medium of the shell is a metamaterial characterized by the relative permittivity $\epsilon_r = -1.0001$, the relative permeability $\mu_r = -1.0001$, and the loss $\nu = 0.0001$.

Figure 2 shows the calculated spatial distribution of the equal-amplitude lines for the total field. There are two regions inside the shell where the field amplitude maxima are localized. One region is located along the line $\varphi = \pi$, and the other, along two curved lines enveloping the illuminated segment of the interior cylinder. Beyond the structure, the field amplitude maxima are situated along the line $\varphi = \pi$. The amplitudes of these maxima decrease as the distance from the outer boundary of the shell grows. In addition, the distribution of the field amplitude in this region indicates that the shell is an omnidirectional scatterer of the incident field.

In order to interpret this distribution of field amplitude maxima, let us consider the results obtained with the use of the GO approximation. Obviously, in the case of such a scatterer, the GO rays refracted by the outer boundary of the shell can be divided into two sets. The first set includes the GO rays that are refracted by the outer boundary of the shell, do not fall on the surface of the interior cylinder, and, hence, are

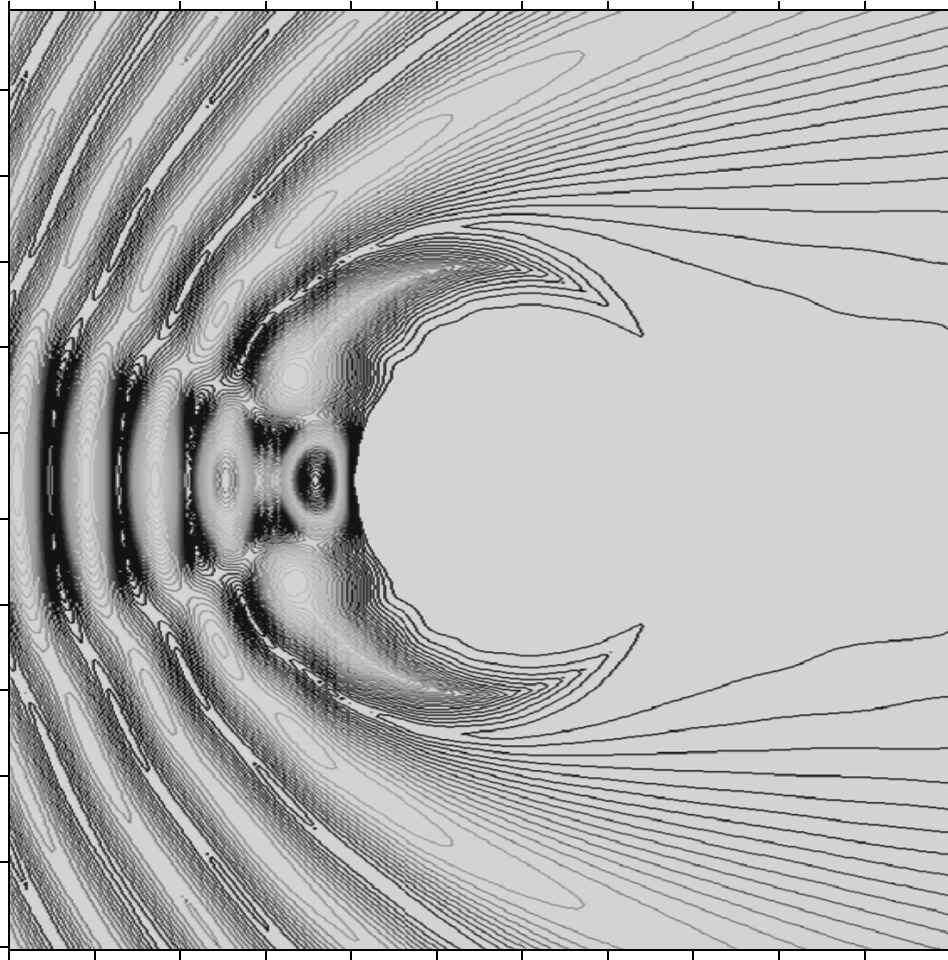


Fig. 2. Spatial distribution of equal-amplitude lines for the total field. The results are obtained for the shell's thickness $kd = 4$, $n_r = -1.0001$, and a plane incident wave.

not reflected by it. The second set of GO rays consists of the GO rays that are refracted by the outer boundary of the shell, fall on the surface of the interior cylinder, and are reflected by it. Depending on the electric dimensions of the scatterer, each set of the GO rays can form various types of caustics. Examples of GO ray trajectories inside the shell with the aforementioned parameters are calculated for these two sets and presented in Figs. 3a and 3b, respectively. It is seen from Fig. 3a that, for the considered geometry of the shell, the first GO ray set forms two separate branches of a smooth caustic. The second GO ray set consists of two subsets. The first subset includes the GO rays that are reflected in the neighborhood of the point with the coordinates $r = a_0$ and $\varphi \approx \pi$ and form a caustic with one cusp point (see Fig. 3b). The second subset includes the GO rays that form no caustic upon reflection from the surface of the interior cylinder. Note that none of the GO ray sets form focus points (i.e., points where all refracted GO intersect) inside the shell. The comparison of Figs. 3 and 2 shows that some of local field maxima are situated just in the neighborhood of

the aforementioned caustics. The rest local field maxima are situated along the line $\varphi = \pi$ and are related with the in-phase and antiphase summation of the GO ray fields incident on and reflected by the surface of the perfectly conducting cylinder for $r = a_0$ and $\varphi = \pi$. Thus, it follows from the ray pattern that the presence of the main field maximum inside the shell is due to the presence of the cusp point of the caustic of the GO rays reflected by the interior cylinder rather than to the existence of the focus point. In addition, the existence and alternation of field maxima on the line $\varphi = \pi$ beyond the structure is explained by the interference of the incident ($\varphi = 0$) and reflected ($\varphi = \pi$) GO rays rather than by focusing.

Now, let the cylindrical wave source have the coordinates $kR_0 = 25$ and $\varphi = \pi$, i.e., be located in the near zone of the shell.

The spatial distribution of equal-amplitude lines calculated for this case is displayed in Fig. 4. The comparison of the data from Figs. 4 and 2 shows that taking into account the curvature of the incident wave front

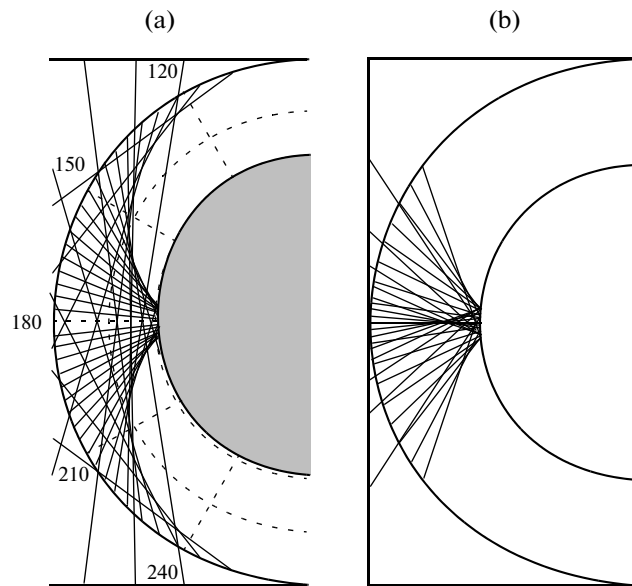


Fig. 3. Pattern of two sets of refracted GO rays inside a shell whose medium has the refractive index $n_r = -1.0001$.

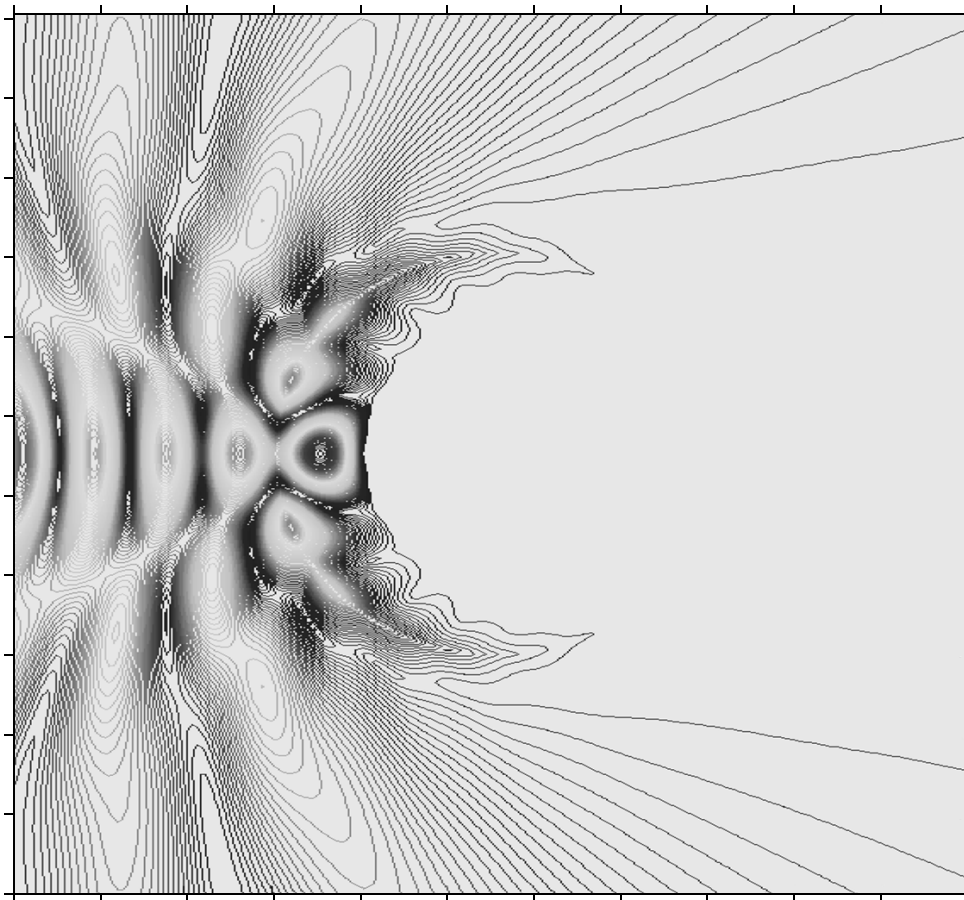


Fig. 4. Spatial distribution of equal-amplitude lines for the total field. The results are obtained for the shell's thickness $n_r = -1.0001$, $kd = 4$, and a cylindrical incident wave.

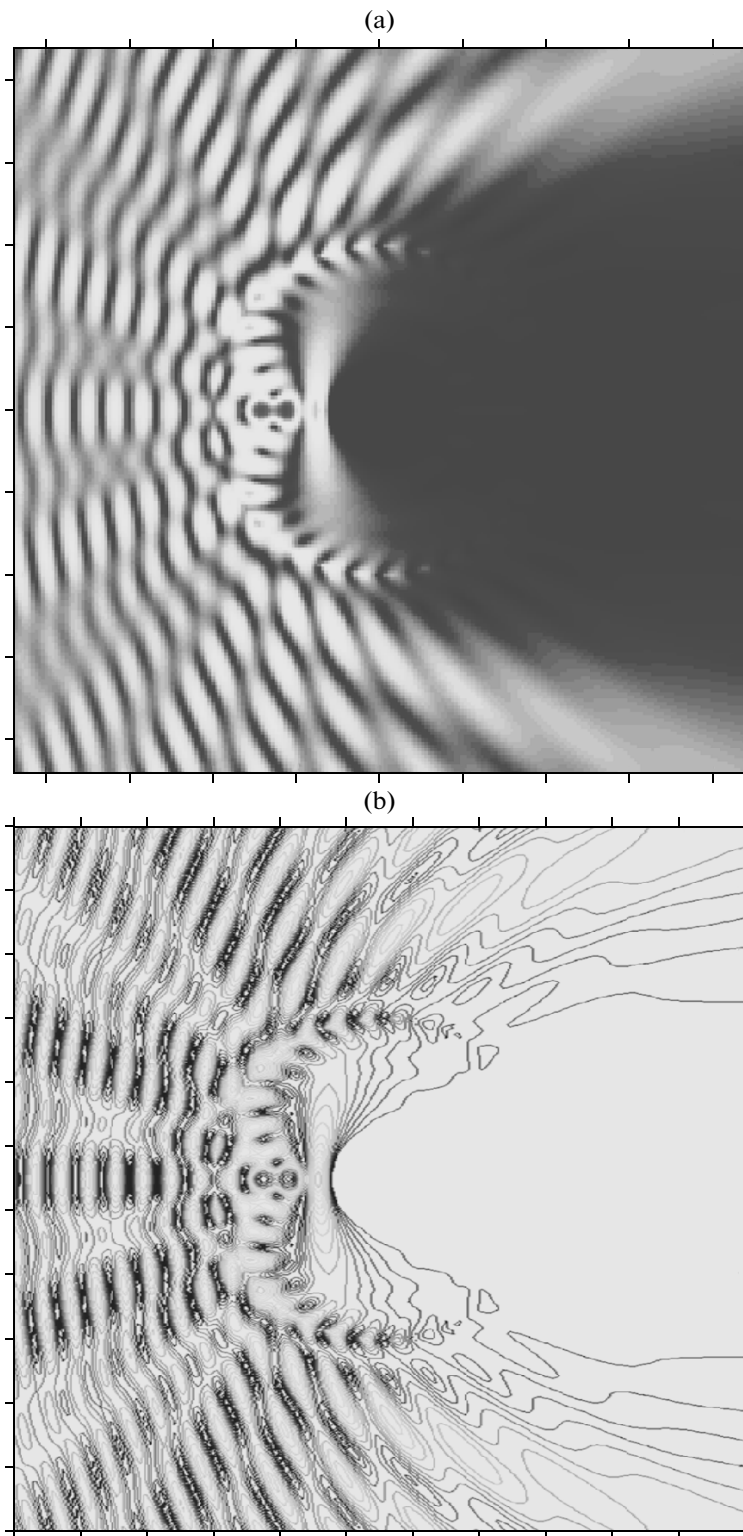


Fig. 5. Spatial distribution of the (a) total field amplitude and (b) equal-amplitude lines for the total field. The results are obtained for the shell's thickness $kd = 14$, $n_r = -1.0001$, and a plane incident wave.

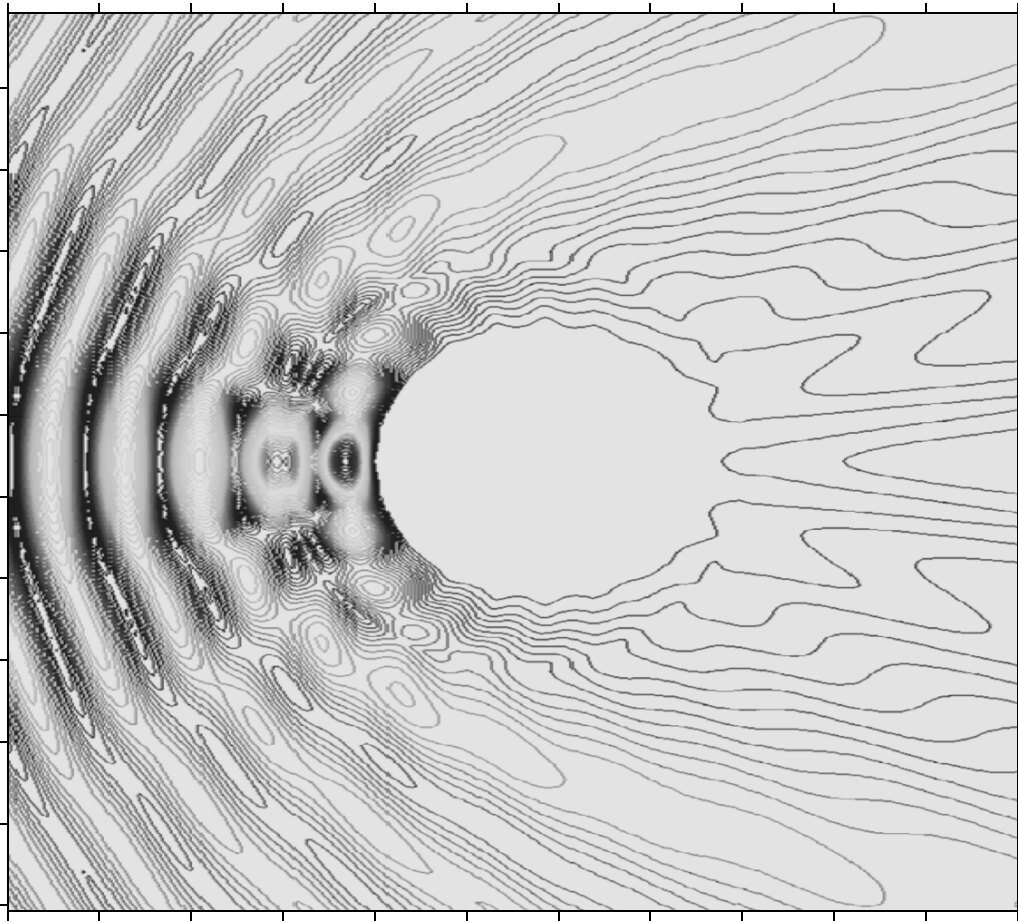


Fig. 6. Spatial distribution of equal-amplitude lines for the total field. The results are obtained for the parameters of the shell's medium $\varepsilon_r = -1.4$ and $\mu_r = -1.3$ and a plane incident wave.

changes the position of the main maximum of the field amplitude in the exterior of the shell: this maximum shifts from the shell toward the source rather than being situated near the shell. The general character of the field focusing in the interior of the shell is retained.

Now, let us consider the influence of the shell thickness on the structure of the scattered field. Within the framework of GO, the structure of the GO ray set and the presence and geometry of caustics substantially depend on the geometry of the problem. In particular, it seems evident that an increase in the shell's thickness kd should mainly affect the structure of the refracted GO rays that are not reflected by the interior cylinder. It follows from the results of studies [18, 19] (where the problem of diffraction of plane and cylindrical waves by an electrically thick cylinder and a metamaterial shell is investigated) that the GO rays refracted by (transmitted through) the outer boundary of the scatterer form a caustic with one cusp point. Therefore, it should be expected that an increase in thickness kd of the metamaterial layer covering the metal cylinder will lead to field focusing inside the shell on two caustics, each having one cusp point. This

effect is illustrated by the calculated spatial distributions of the field amplitude and equal-amplitude lines for the field that are depicted in Figs. 5a and 5b, respectively. In the calculation, it is assumed that the electric radius of the outer surface of the shell is $ka = 20$ and, hence, the shell's thickness is $kd = 14 \gg 1$. The remaining parameters of the problem coincide with the data of the problem considered above. It follows from the results presented in Fig. 5 that the field in the interior of the shell is localized on two caustics. The first caustic has one cusp point and is formed by the GO rays that are refracted by the outer boundary of the shell and do not fall on the interior perfectly conducting cylinder. The second caustic has one cusp point and is formed by the GO rays reflected by the interior cylinder.

Now, let us consider the influence of the refractive index on the structure of the near field of a metal cylinder covered by a metamaterial shell. Assume that a perfectly conducting cylinder has the electric radius $ka_0 = 6$ and is covered by a cylindrical metamaterial shell with the relative permittivity $\varepsilon_r = -1.4$, the relative permeability $\mu_r = -1.3$, and the loss $\nu = 0.0001$.

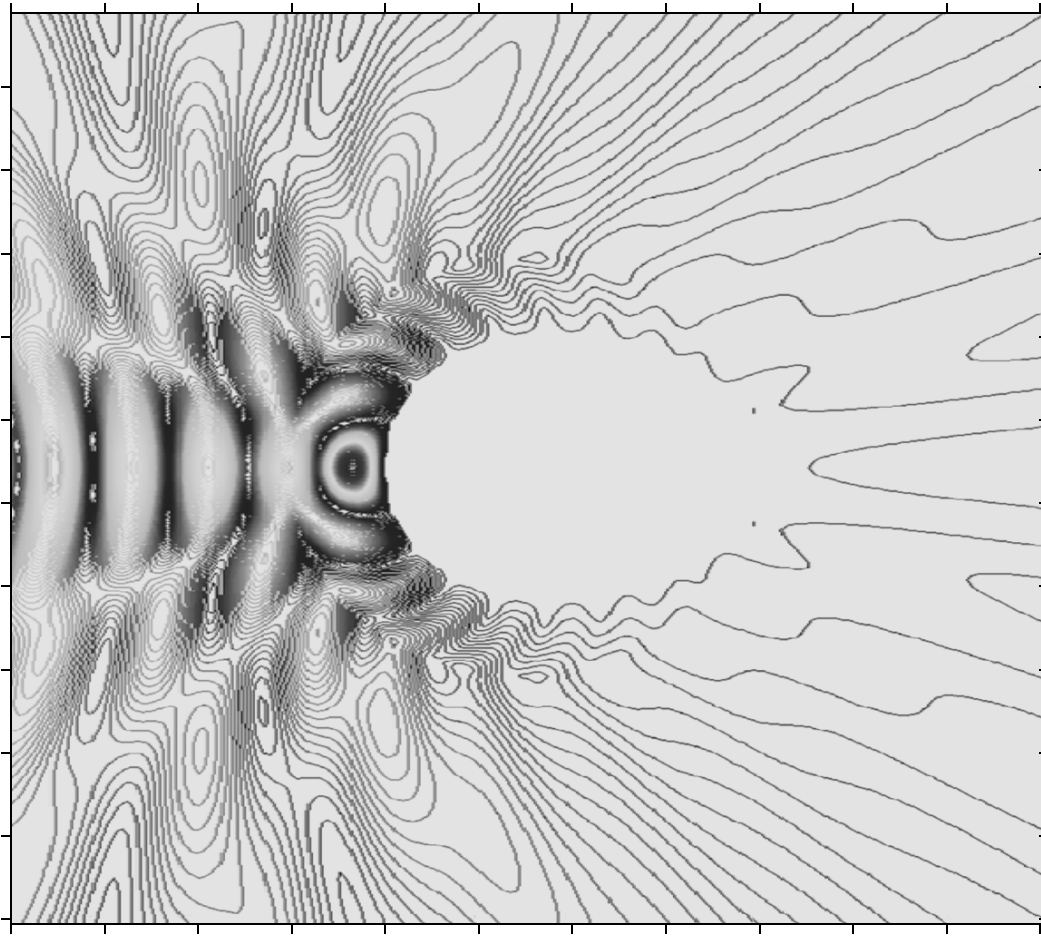


Fig. 7. Spatial distribution of equal-amplitude lines for the total field. The results are obtained for the parameters of the shell's medium $\varepsilon_r = -1.4$ and $\mu_r = -1.3$ and a cylindrical incident wave.

The outer electric radius of the shell is $ka = 10$. The coordinates of a cylindrical wave source are $kR_0 = 700$ and $\varphi_0 = \pi$. Physically, this means that we deal with the case of diffraction of a plane wave by an electrically thin shell.

Figure 6 shows the spatial distribution of equal-amplitude lines for the field calculated for this case. As in the foregoing, here, $|n_r| = \sqrt{|\varepsilon_r| |\mu_r|} \approx 1$ (see Fig. 2) and we can notice field focusing on the aforementioned two types of caustics. We deal with the situation when the field focusing on two caustic branches is pronounced more distinctly than in the case illustrated in Fig. 2. In addition, the effect of field leaking into the shadow region is observed.

Let us place the cylindrical wave source at the point with the coordinates $kR_0 = 25$ and $\varphi = \pi$. The rest parameters of the problem are retained. The spatial distribution of the field amplitude calculated for this case is depicted in Fig. 7. It is seen from this figure that the field distribution in the interior of the shell substantially differs from that observed in the case of the diffraction of the plane wave. Thus, the process of field

leaking into the shadow region has a wave-like character, a circumstance that is not observed in Fig. 6.

Now, let the medium of the metamaterial shell be characterized by the relative permittivity $\varepsilon_r = -0.5$, the relative permeability $\mu_r = -0.5$, and the loss $\nu = 0.0001$. The remaining parameters are retained. The spatial distribution of equal-amplitude lines calculated for the cases of the incidence of plane and cylindrical waves are presented in Figs. 8a and 8b, respectively. The coordinates of the wave source are $kR_0 = 25$ and $\varphi_0 = \pi$. It is seen that, for the field inside the shell, the caustics of refracted GO rays (i.e., the rays that are refracted by the outer boundary and do not fall on the interior metal cylinder) are so closely spaced from the outer boundary that, actually, the field is not focused on it. In the case of a cylindrical incident wave, the region into which the refracted field leaks is reduced.

Thus, it follows from the results presented above that the character of diffraction of a plane (cylindrical) wave by a perfectly conducting cylinder that has large electric dimensions and is covered by a metamaterial

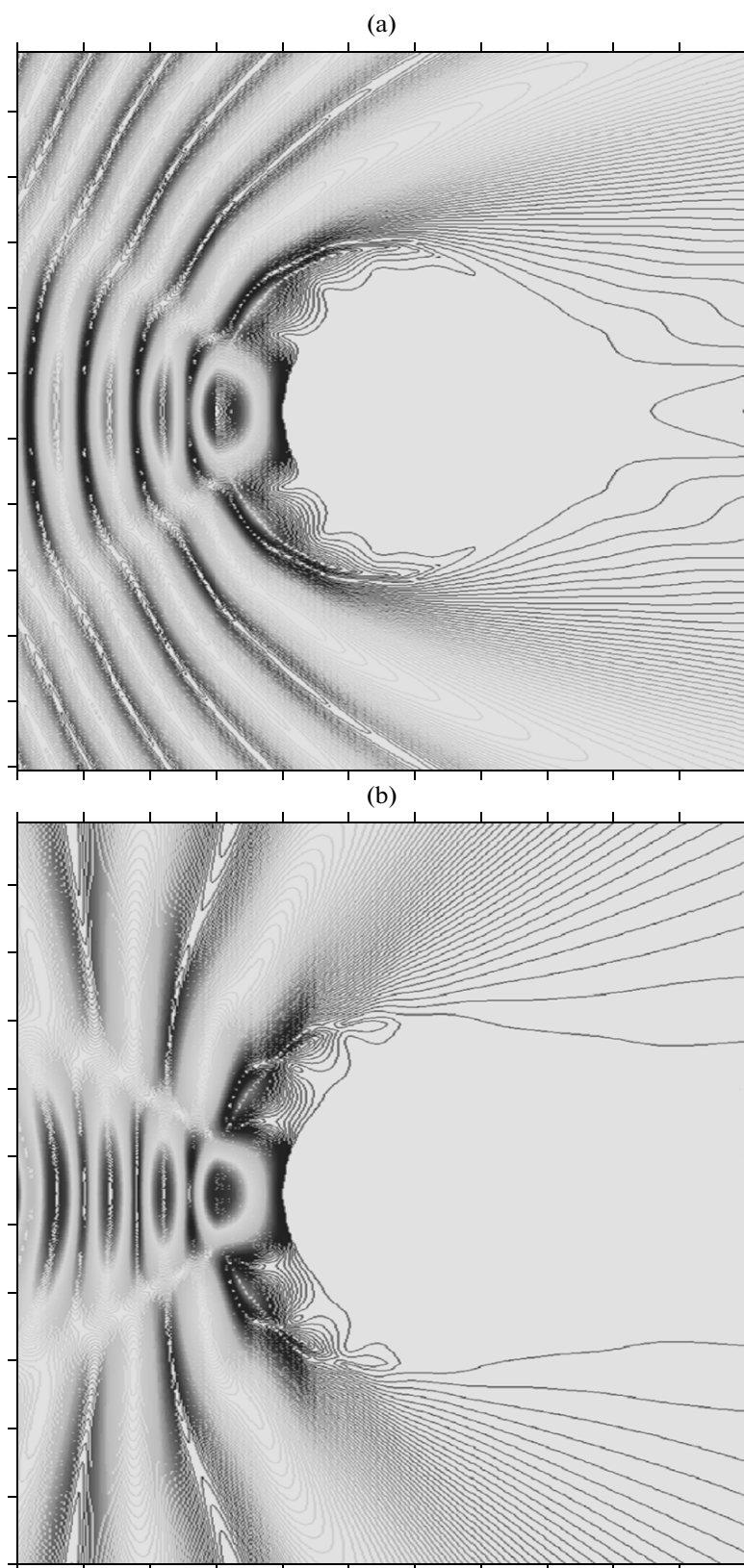


Fig. 8. Spatial distribution of equal-amplitude lines for the total field. The results are obtained for the refractive index of shell's medium $n_r = -0.5$ and (a) plane and (b) cylindrical incident waves.

layer is related with focusing of the refracted field on two caustics. Each of the caustics can have one cusp point. The case when the electric dimensions of such a scatterer are commensurable with the wavelength calls for additional consideration.

ACKNOWLEDGMENTS

This study was supported by the Russian Foundation for Basic Research, project nos. 10-02-01103 and 12-02-00062.

REFERENCES

1. V. G. Veselago, Usp. Fiz. Nauk **92**, 517 (1967).
2. J. B. Pendry, Phys. Rev. Lett. **85**, 3966 (2000).
3. A. Sihvola, Metamaterials **1** (1), 2 (2007).
4. V. Veselago, L. Braginsky, and V. Shklover, and C. J. Hafner, J. Comput. Theor. Nanosci. **3**, 189 (2006).
5. N. V. Kisel' and A. N. Lagar'kov, Elektromagn. Volny Elektron. Sist. **7** (7), 55 (2002).
6. A. P. Anyutin, J. Radioelectron, No. 7 (2007); <http://ire/cplire.ru/jre/jul07/5/text.html>.
7. A. D. Shatrov, J. Commun. Technol. Electron. **52**, 842 (2007).
8. A. P. Anyutin, J. Commun. Technol. Electron. **53**, 387 (2008).
9. A. P. Anyutin, J. Commun. Technol. Electron. **53**, 1323 (2008).
10. A. B. Petrin, JETP **106**, 963 (2008).
11. A. P. Anyutin, J. Commun. Technol. Electron. **54**, 982 (2009).
12. V. P. Mal'tsev and A. D. Shatrov, J. Commun. Technol. Electron. **55**, 278 (2010).
13. A. P. Anyutin, J. Commun. Technol. Electron. **55**, 132 (2010).
14. V. A. Borovikov and B. E. Kinber, *Geometric Theory of Diffraction* (Svyaz', Moscow, 1978) [in Russian].
15. A. S. Kryukovskii, D. S. Lukin, and D. V. Rastyagaev, J. Commun. Technol. Electron. **50**, 1129 (2005).
16. A. P. Anioutin, A. G. Kyurkchan, and S. A. Minaev, J. Quant. Spectrosc. Radiat. Transf. **79–80**, 509 (2003).
17. A. G. Kyurkchan, S. A. Minaev, and A. L. Soloveichik, J. Commun. Technol. Electron. **46**, 615 (2001).
18. A. P. Anyutin, J. Commun. Technol. Electron. **56**, 1029 (2011).
19. A. P. Anyutin, J. Commun. Technol. Electron. **58**, 101 (2013).

Translated by I. Efimova